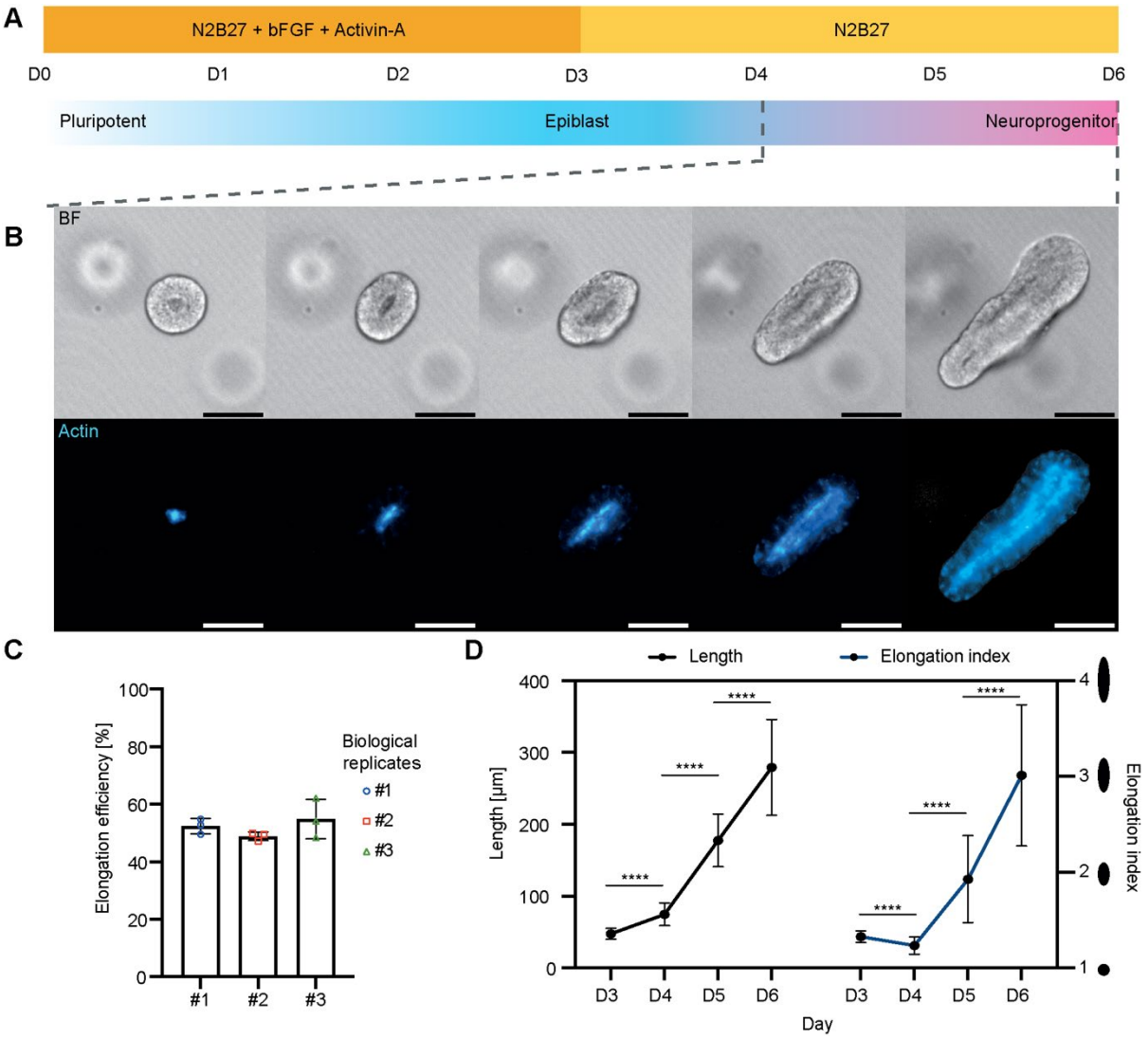


**Fig. S1**. **Generation of self-elongating neural tube organoids in 3D. A**, Schematic representation of self-elongating neural tube organoids culture in 3D. Single mouse ESCs embedded in Matrigel cultured in epiblast medium (N2B27 with Activin-A and bFGF) form epiblast-state cysts on D3. From D3 on, the medium was changed to N2B27 for neural differentiation. On D4, cysts undergo uniaxial elongation and form elongated neural tube-like structure bearing a single and continuous elongated lumen. **B**, Representative time-lapse images capturing the elongation of a neuroepithelial cyst into a tubular structure between D4 and D6. The images were obtained both in brightfield and fluorescence with a live cell actin probe to capture both the elongation of neuroepithelial cysts and their respective lumen. Surprisingly, the apicobasal polarization of the organoid was maintained during elongation. **C**, Elongation efficiency of neuroepithelial cyst of three independent biological replicates. **D**, Quantitative analysis of elongation in length as well as the Elongation index between D3 and D6. All the scale bars are 100 µm.

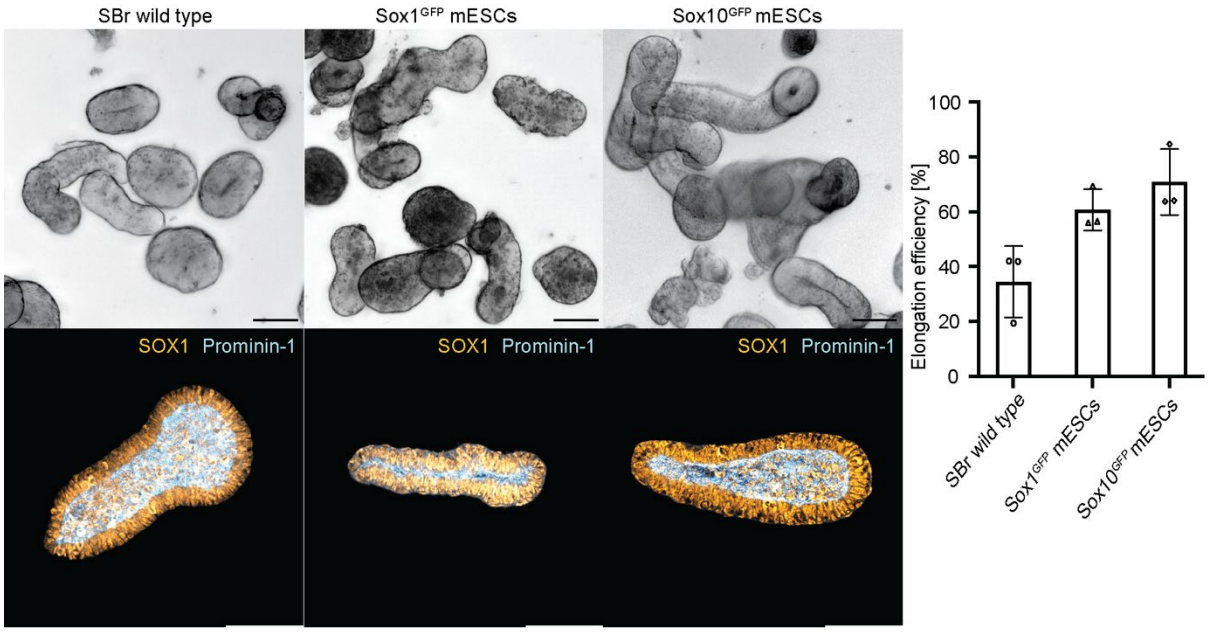


**Fig. S2. Reproducible generation of self-elongating neural tube organoid across different cell lines.** Self-elongating neural tube organoid could be generated in a reproducible manner in three different cell lines: Wild type of SBr cell line (Deluz *et al.*, 2016), *Sox1*$^{GFP}$ mESCs (Aubert *et al.*, 2003; Meinhardt *et al.*, 2014) and *Sox10*$^{GFP}$ mESCs (Kawaguchi *et al.*, 2010). Each cell line has its optimal Matrigel-embedding cell density (Table 1) and their efficiency of elongation is about 55.34 ±18.92% in average.

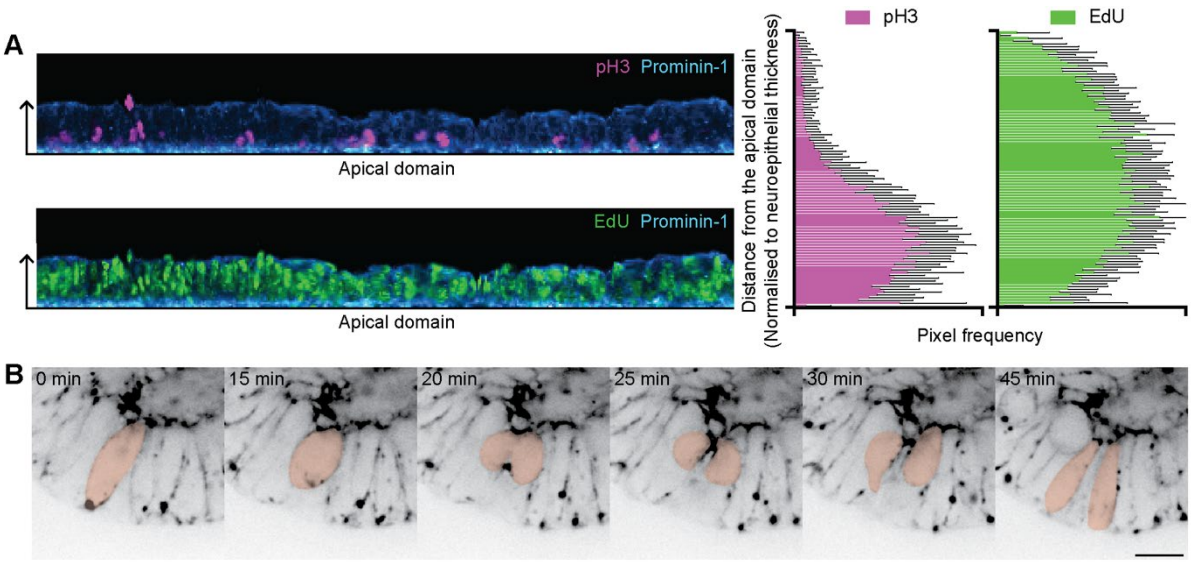


**Fig. S3. Interkinetic nuclear migration is exhibited in the neural tube organoid. A**, straightened image of epithelium of neural tube organoid stained against pH3 (M-phase cell) and EdU (S-phase cell) showed the apically localised M-phase mitotic cells. The quantification of the pixel frequency of $pH3^{+}$ or $EdU^{+}$ signal along the thickness of the epithelium show the biased localisation of mitotic cells at the apical domain of the organoid (n=22). **B**, timelapse of the organoid stained with live actin could capture interkinetic nuclear migration and their cell division at the apical domain. Scale bar is 20 μm.

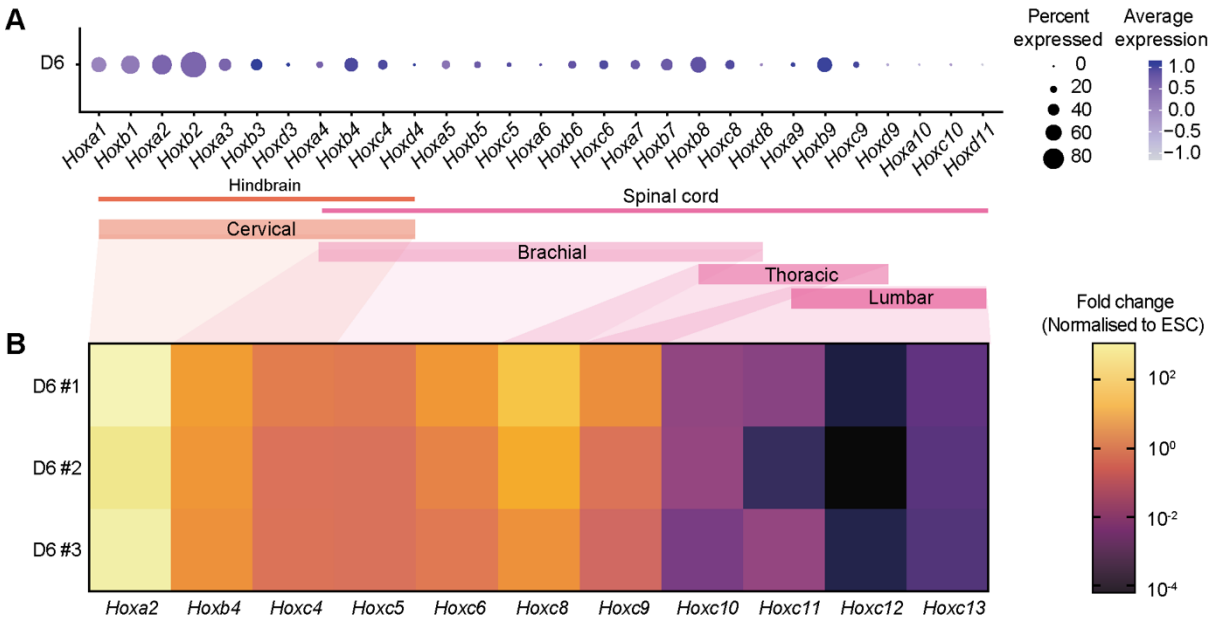


**Fig. S4. Hox gene expression in neural tube organoid. A**, Dot plot showing Hox genes and their expression level in neural tube organoids on D6. The percentage of cells expressing anterior Hox genes is larger but shows lower expression levels, whereas posterior Hox genes are expressed in fewer cells but these show higher expression level. The range of Hox gene expression spans between the cervical level (hindbrain) to the beginning of lumbar level (spinal cord). **B**, Reproducible Hox gene expression in three biological replicates of D6 neural tube organoids analyzed by qPCR also range from cervical to lumbar neural tube levels.

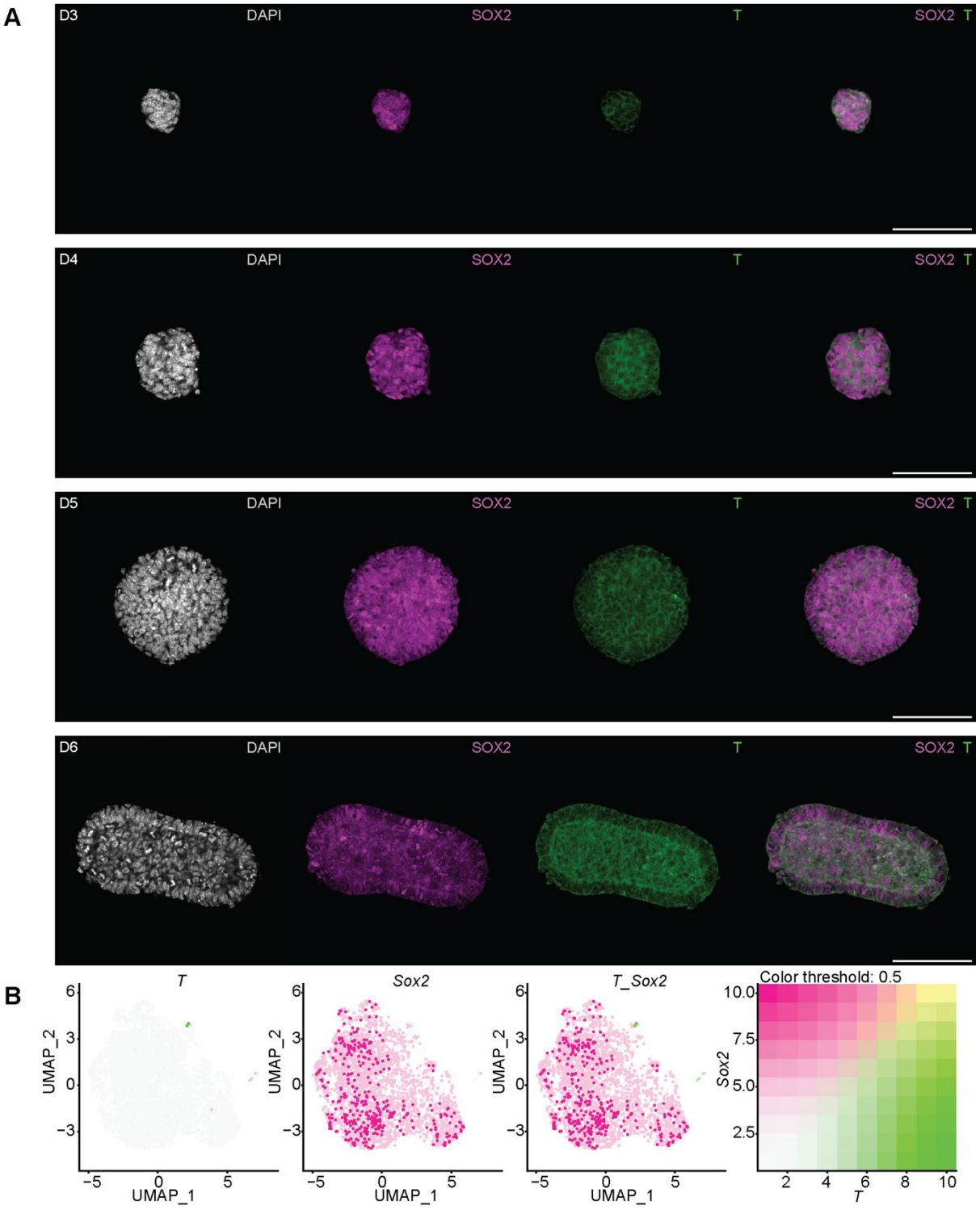


**Fig. S5. Neuromesodermal progenitor (NMP) was not detected in neural tube organoid. A**, Immunostaining of neural tube organoid against T (mesodermal) and SOX2 (neural) on D3 to D6 shows that there is no NMP ($T^+$ $SOX2^+$) detected in the organoid. **B**, scRNAseq analysis did not detect any NMP ($T^+$ $SOX2^+$) population in the organoid on D6. The UMAP plots were generated from the same data set analysis of Fig. 2.

Supplementary Figure 6

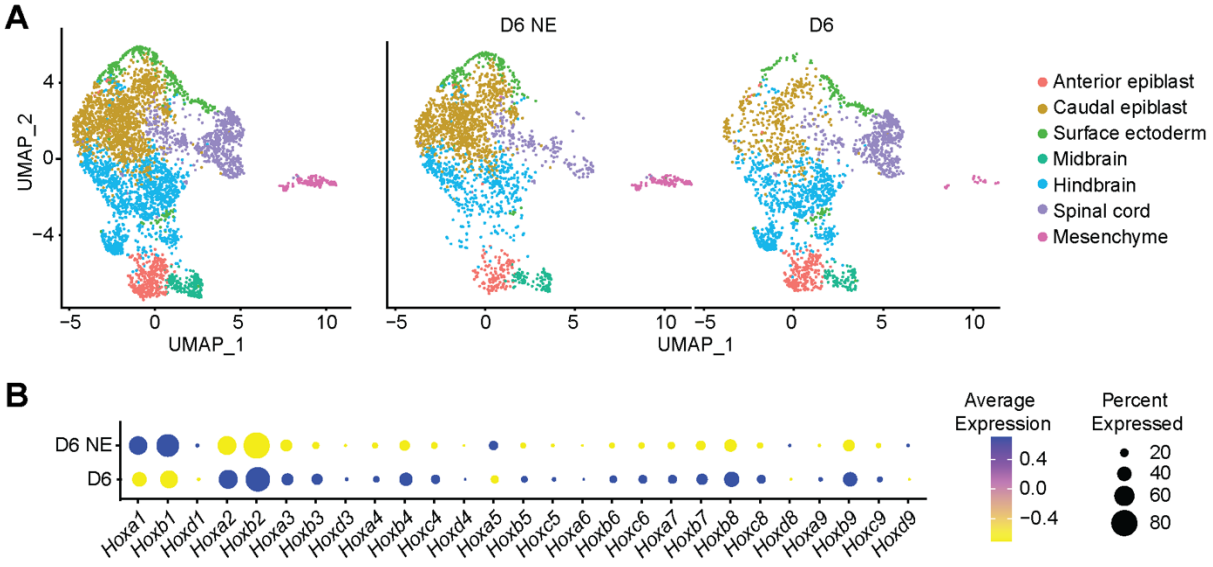


**Fig. S6. Comparison between self-elongated neural tube organoid (D6) and non-elongated neural tube organoid (D6 NE) using scRNAseq. A**, D6 and D6 NE shares all the cell types but the neural progenitors with spinal cord identity are preferentially found in self-elongated organoid. **B**, Dotplot of Hox genes along AP axis shows that D6 organoids express Hox genes along the AP axis from Hox2 level to Hox9 level while D6 NE organoids express anterior Hox gene restrictedly.

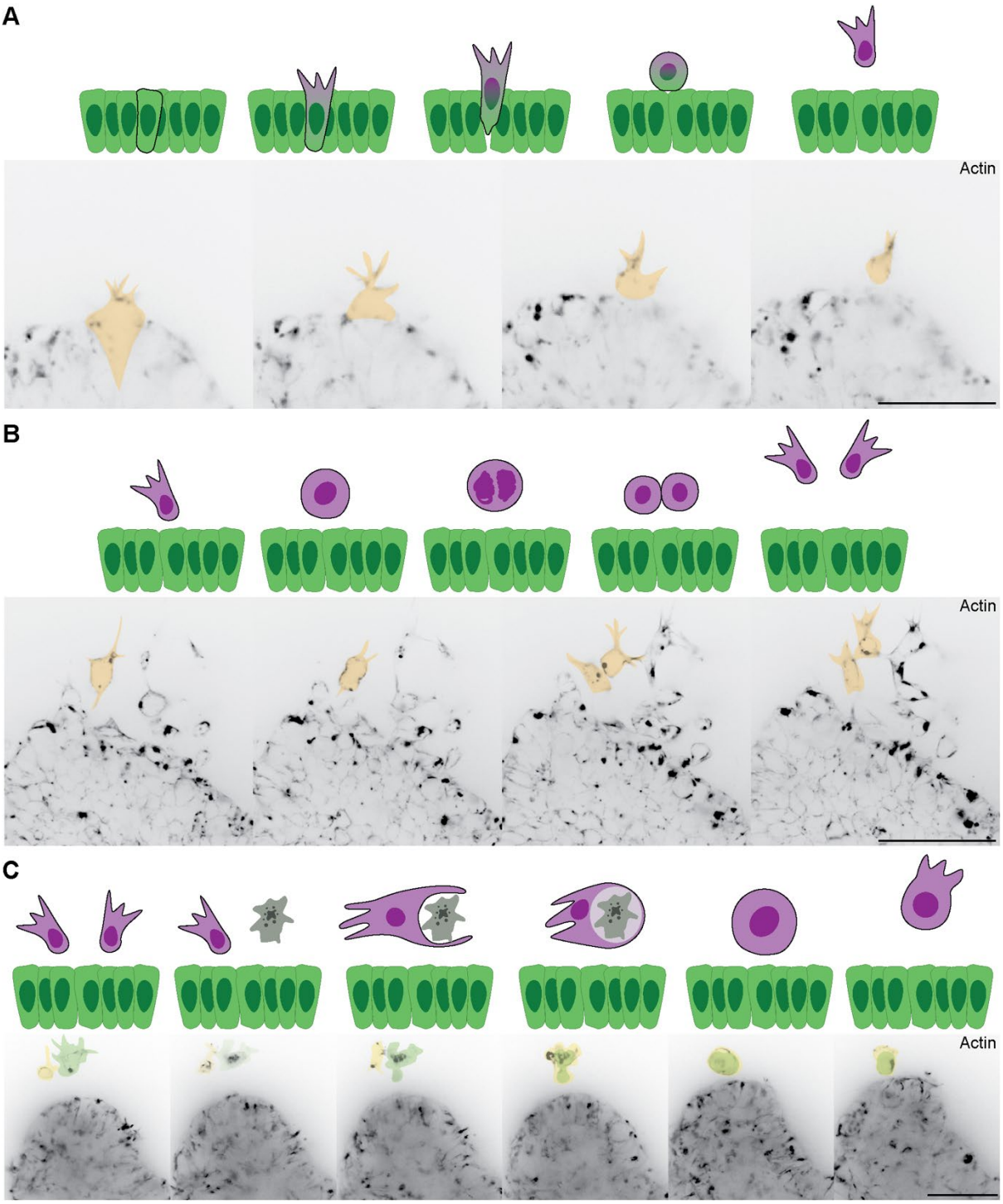


**Fig. S7. Real-time observation of neural crest cell emergence. A**, Delamination and migration of neural crest cells. The schematic and the time-lapse images depict the process of delamination and migration of the neural crest cells emerged from neural tube organoid. First, the cell protrudes out its filopodia out of the neuroepithelium and changes its morphology to go on the surface of the neuroepithelium. Then, the cell is entirely separated from the neural tube organoid and migrate away from the organoid having the filopodia towards the direction of migration. **B**, Self-renewal of migratory neural crest cells. The schematic and the time-lapse images show the self-renewal of migratory neural

crest cell. C, Phagocytosis of migrating neural crest cells. The schematic and the time-lapse images demonstrate the phagocytosis of migrating neural crest cells. When there was an apoptotic cell, the neighbouring migratory neural crest cell migrated towards the apoptotic debris, engulfed, and continued migrating. All the scale bars are 50 μm.

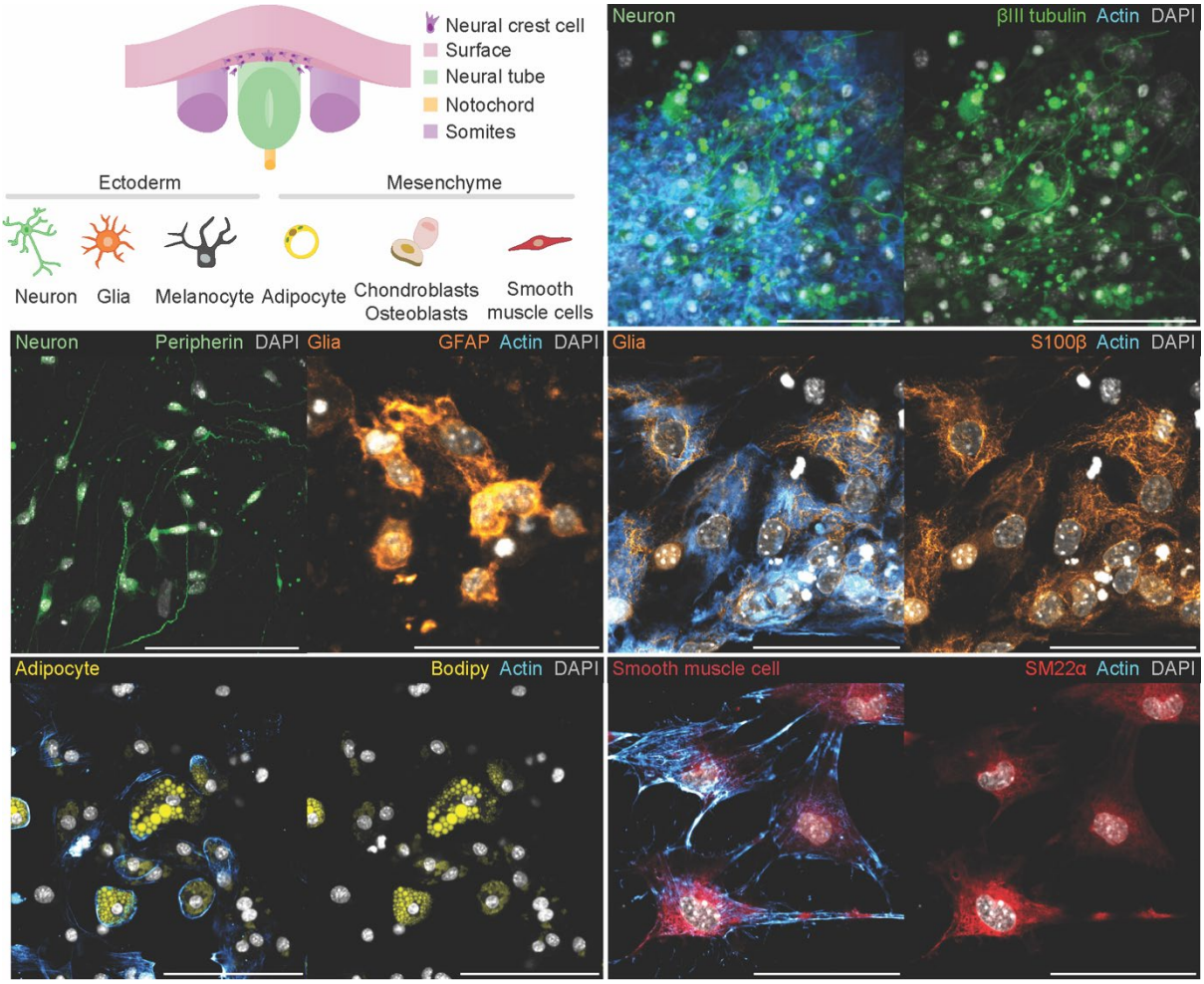


**Fig. S8. Multipotency of neural crest cells derived from mature neural tube organoid.** Neural crest cells can be derived into ectodermal cells, such as neuron and glia, and mesenchymal derivatives, such as adipocyte and smooth muscle cells. Culturing the neural tube organoid for a month revealed the multipotency of the neural crest cells. Confocal imaging confirmed that the neural crest cells have differentiated into various cell types: neurons expressing βIII tubulin, glial cells expressing GFAP and S100β, mesenchymal derivatives like adipocyte with the lipid droplets visualized by Bodipy and smooth muscle cells expressing SM22α. All the scale bars are 50 μm.

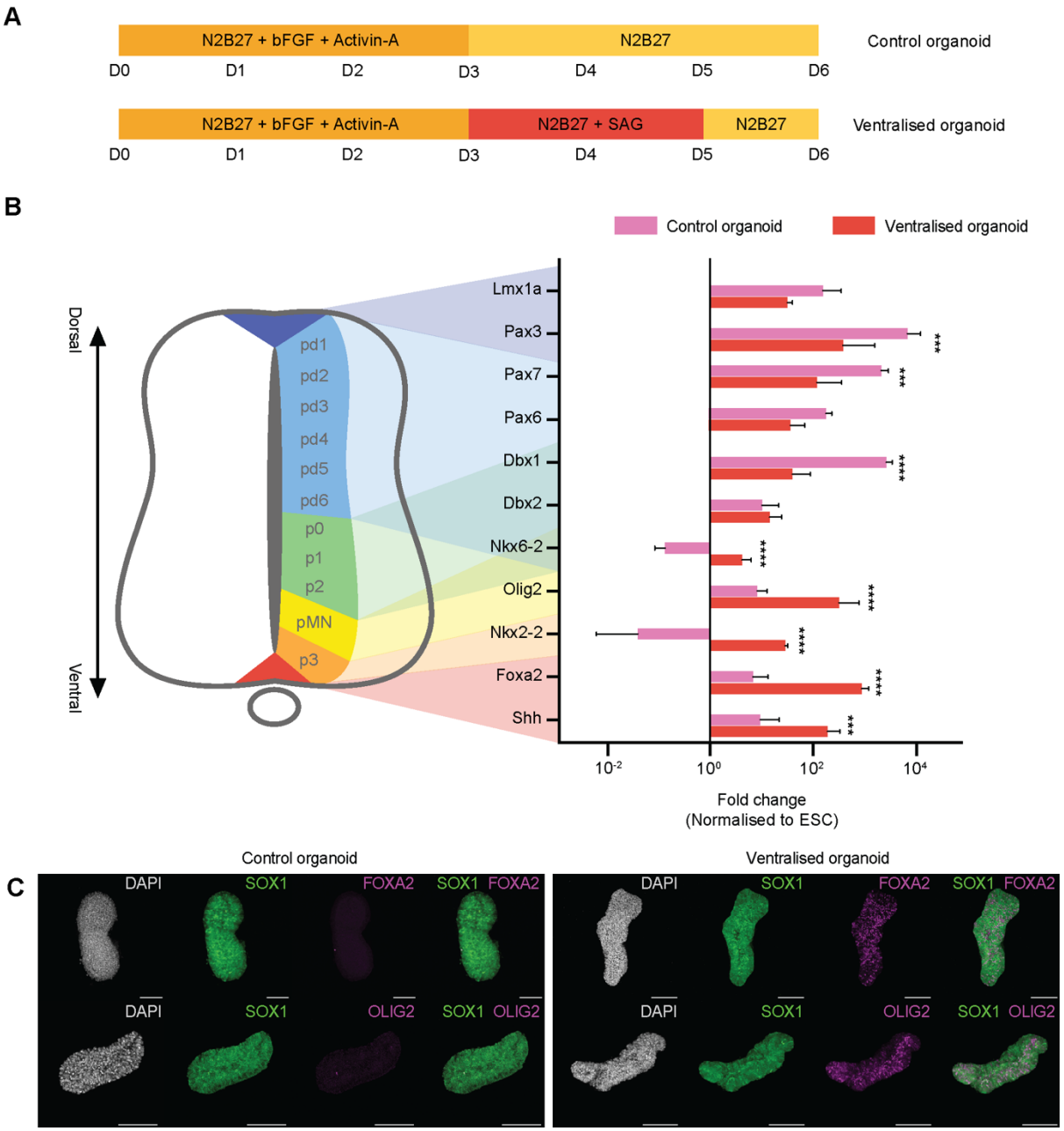


**Fig. S9. Ventral morphogen can induce ventral identity cell types in the organoid. A**, Schematic representation of the protocol used to ventralise the organoids. After culture in epiblast medium, control neuroepithelial cysts are cultured in N2B27 or in N2B27 with supplemented with 500 nM smoothened agonist (SAG, SHH signalling pathway activator) between D3 and D5 to ventralise the organoid. **B**, qPCR analysis of dorsal-ventral patterning markers of the embryonic neural tube, in control organoid and ventralised organoids. Control organoids show high expression of dorsal markers and low expression of ventral markers, while ventralised organoids show strong upregulation of ventral markers and also retain substantial expression of dorsal markers. This result shows that the organoid has default dorsal fate until ventral morphogen was treated. Values are mean ±SEM. Statistical analysis by 2-way ANOVA with Sidak's multiple comparisons test, ***p<0.001, ****p<0.0001. **C**, Confocal imaging revealed the predominant presence of ventral marker FOXA2 and OLIG2 at the protein level in ventralised organoids comparing to control organoids. This result suggests that selective dorsal or ventral fate of neural tube organoids can be obtained by following according culture condition. All the scale bars are 100 μm.

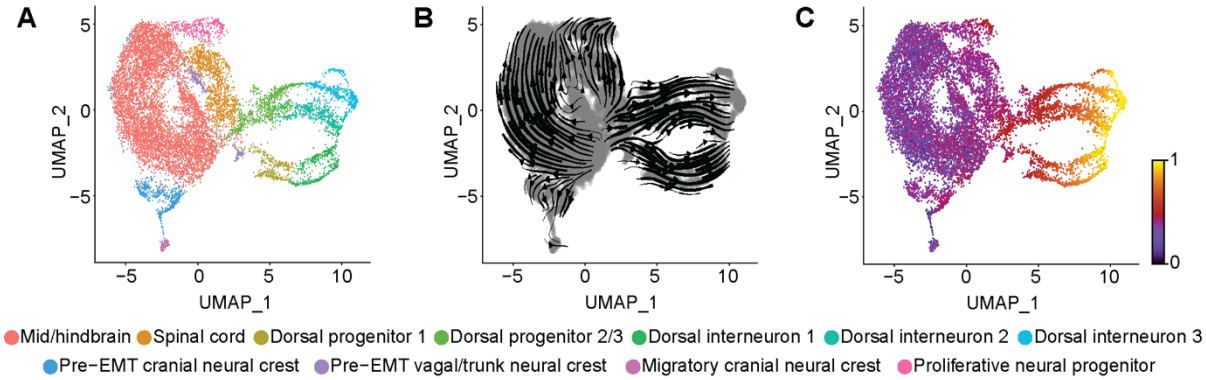


**Fig. S10. RNA velocity analysis aligns with the maturation of the neural tube organoid. A**, scRNAseq of the maturing organoids from D6 to D10 revealed 11 cell type clusters throughout the maturation including dorsal progenitors, dorsal interneurons, and neural crest cells (n= 11,981, N=1 biological sample for each timepoint). **B**, Streamline of RNA velocity displays the developmental process of maturation of neural tube organoid. **C**, Velocity pseudotime computed by RNA velocity aligns with temporal profile of the samples from D6 to D10 on UMAP projection. All the plots were generated from the same data set analysis of Fig. 4.

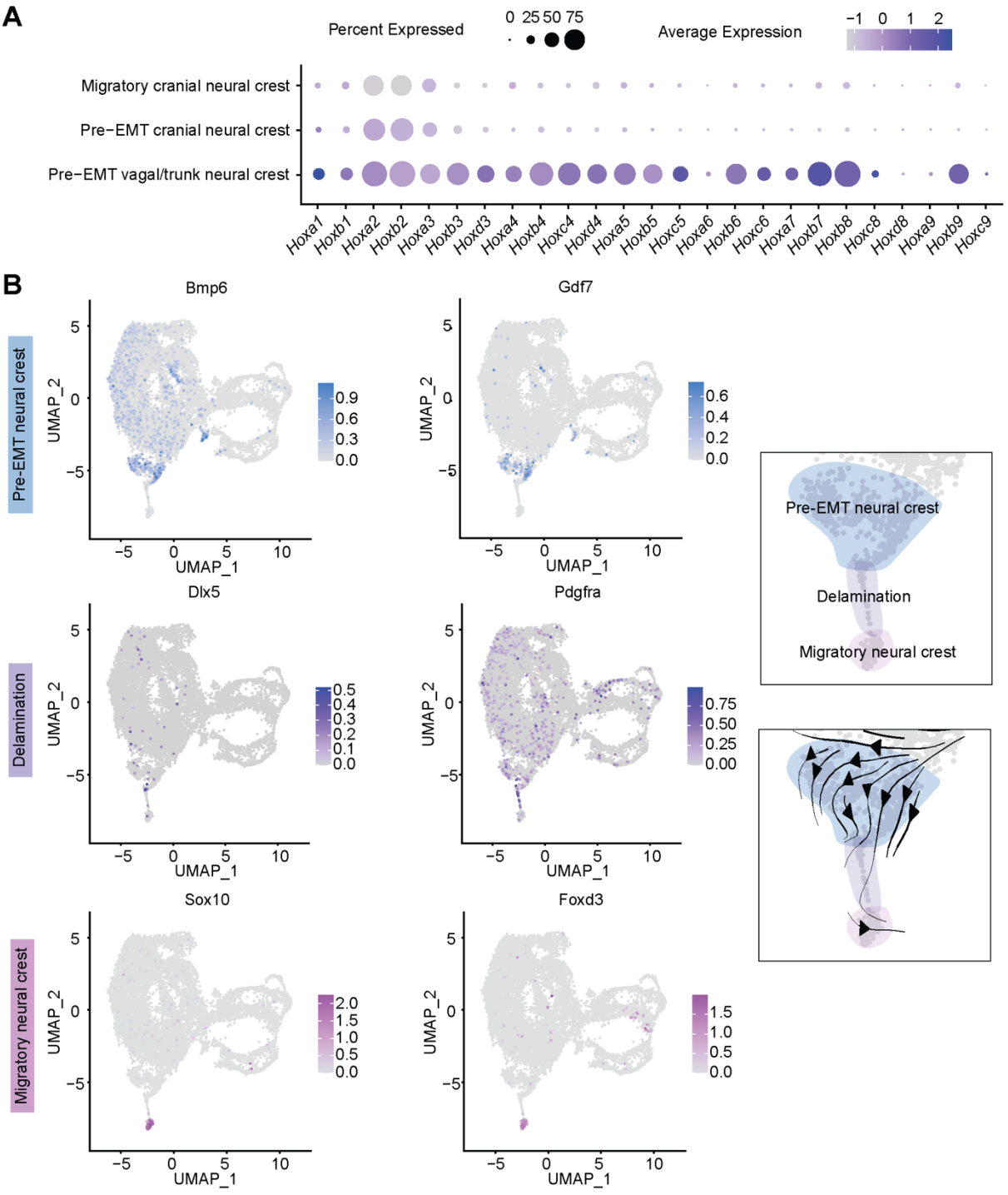


**Fig. S11. scRNAseq analysis of mature neural tube organoids from different timepoint captured the transcriptomic event in neural crest cells from emergence to migration and their regional identity. A**, The expression of Hox genes differentiates the Pre-EMT vagal/trunk neural crest cell from the Pre-EMT cranial neural crest cells. were detected in mature neural tube organoid. The migratory neural crest cells that were spotted migrating out from the organoid are cranial neural crest cells as they are lack of Hox gene expression. **B**, Plotting of the markers of each step: Pre-EMT neural crest (*Bmp6*$^{+}$ *Gdf7*$^{+}$), Delamination (*Dlx5*$^{+}$, *Pdgfra*$^{+}$), and Migratory neural crest cells (*Sox10*$^{+}$, *Foxd3*$^{+}$) captured the

emergence, delamination, and migration of neural crest cells derived from neural tube organoid. The RNA velocity streamlines support this transcriptomic event from preEMT state to delamination and migration. All the plots were generated from the same data set analysis of Fig. 4.

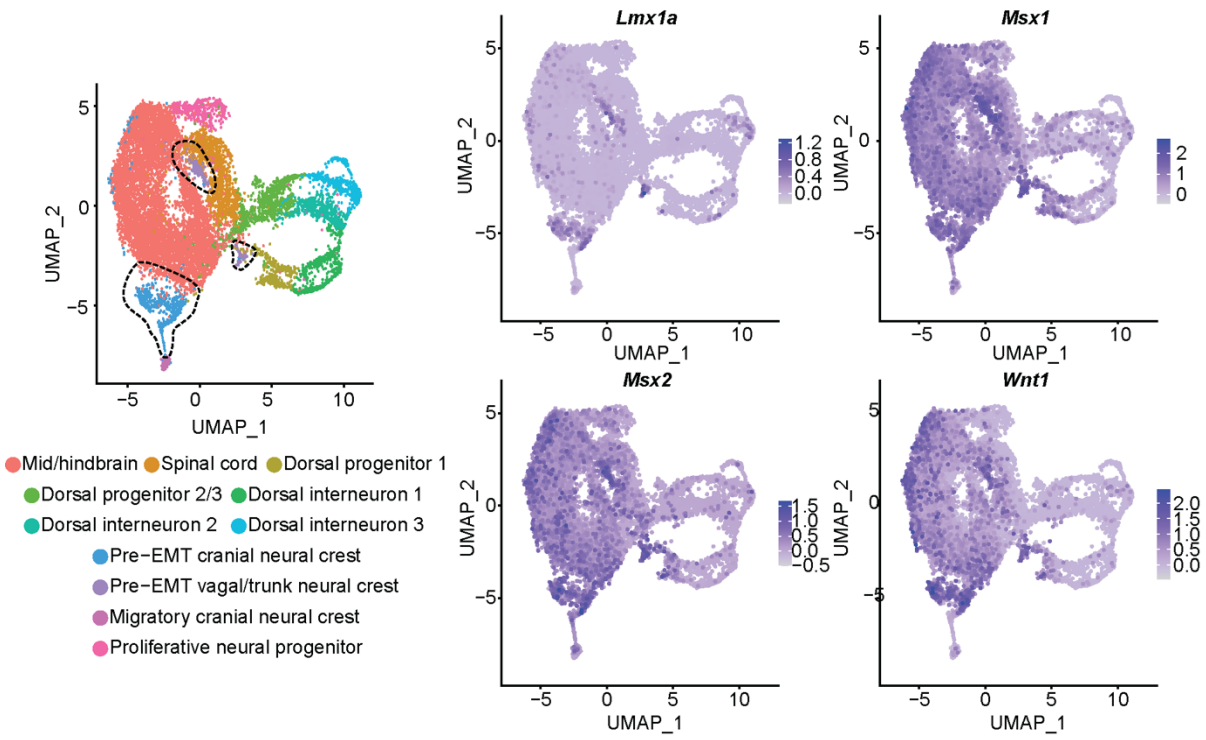


**Fig. S12. Neural crest cells emerge from the roof plate-fate cells in the neural tube organoid.** Roof plate markers, *Lmx1a*, *Msx1*, *Msx2*, and *Wnt1*, were distinctively expressed in the Pre-EMT neural crest clusters (both cranial and vagal/ trunk neural crest, in dotted circles). This result indicates that the neural crest cells emerge from the roof plate-fate cells in neural tube organoids which aligns with the neural crest development *in vivo* where the neural crest cells emerge from the roof plate of the neural tube. All the plots were generated from the same data set analysis of Fig. 4.

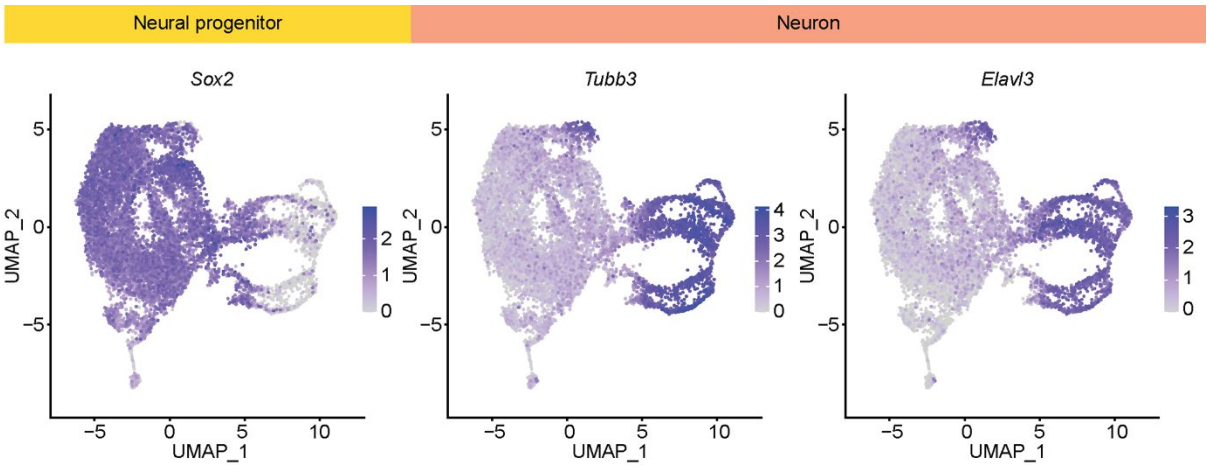


**Fig. S13. scRNAseq captured the transcriptomic event of neural differentiation from neuroprogenitor to neurons.** The cells from D6-D7 organoids were mostly neural progenitor expressing *Sox2* and then were differentiated into more mature neurons expressing *Tubb3* and *Elavl3* by D10. All the plots were generated from the same data set analysis of Fig. 4.


**Movie 1. Self-elongation of the neural tube organoid.** The organoids were stained with live cell actin probe to visualize the lumen and the actin in general of the organoids. **Part 1**, Time-lapse imaging from D0 to D6 showing the self-elongating neural tube organoid formation from a single cell with 10X air objective on Nikon Eclipse Ti inverted microscope. **Part 2**, Time-lapse imaging between D4 and D6 with 1 hour of interval with 10X air objective on Nikon Eclipse Ti Inverted Microscope. **Part 3**, Time-lapse imaging between D5 and D6 with 5 min of interval with 60X oil objective on Visitron CSU-W1. Those time-lapses revealed that the neural tube organoid self-elongate and its lumen elongate simultaneously keeping the neural canal-like structure.

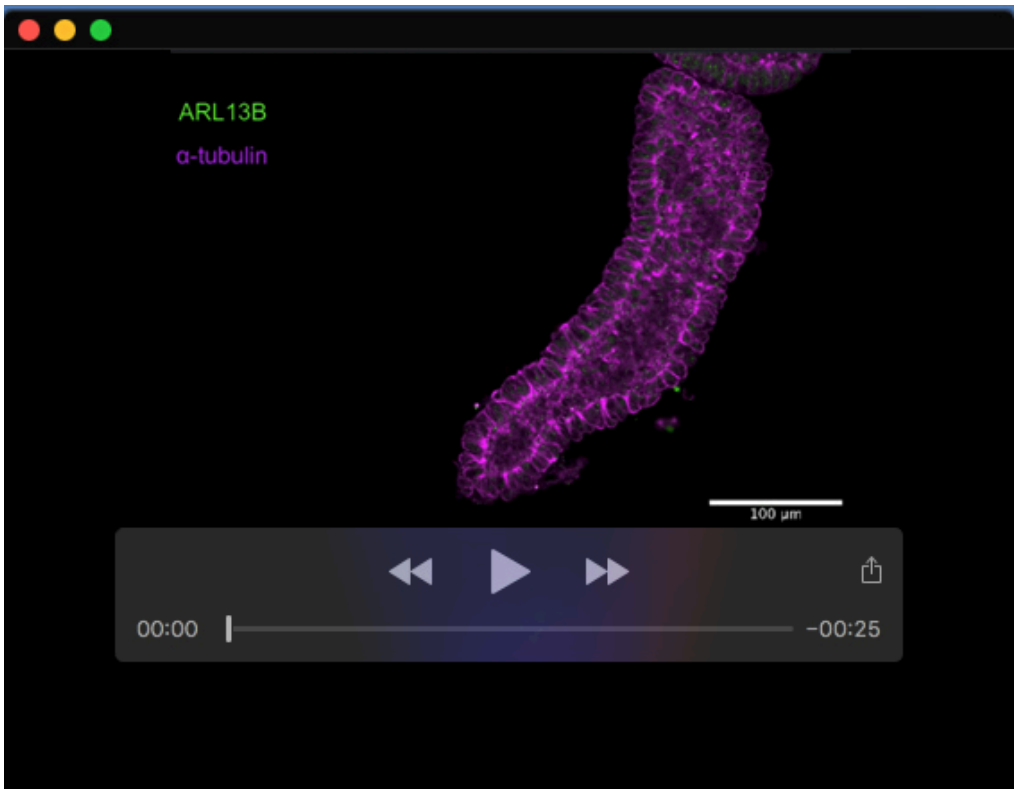


**Movie 2. Primary cilia in the neural tube organoid.** The organoids from D6 were immunostained against ARL13B (primary cilia) and acetylated α-tubulin and the confocal images were taken by Zeiss LSM 700 Inverted Microscope with 20X air or 63X oil objective. This result shows the primary cilia expressing ARL13B are localised at the apical membrane of the neural tube organoid which resembles the neural tube *in vivo*.

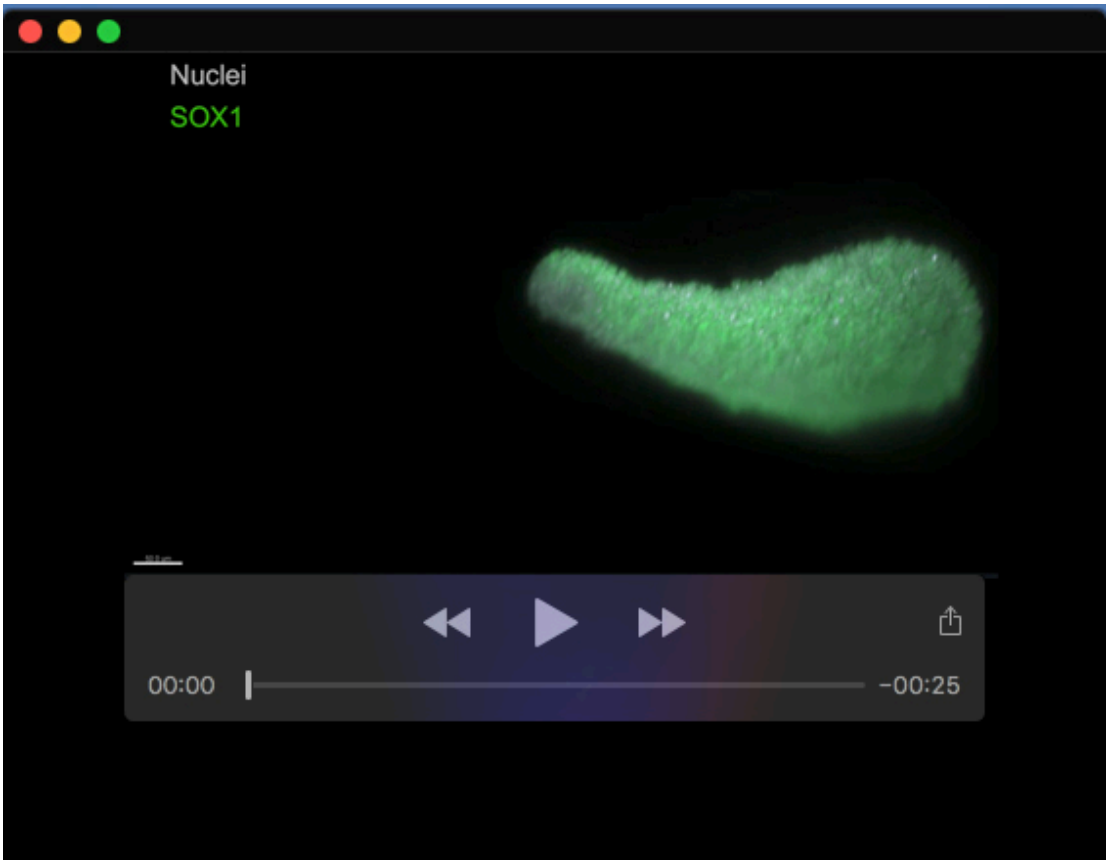


**Movie 3. Neural canal-like structure in neural tube organoid.** The organoids from D6 were stained against SOX1 (neuroectoderm), Ki67 (proliferating cell), and actin and the images were taken by Zeiss Lightsheet Z1 with 20X water objective. 3D projection of the images (IMARIS, Bitplane) clearly shows the actual tubular structure of the organoid with the hollow and elongated lumen in the middle of the neural tube organoid that recapitulates the neural canal *in vivo*. Scale bar is 50 μm.

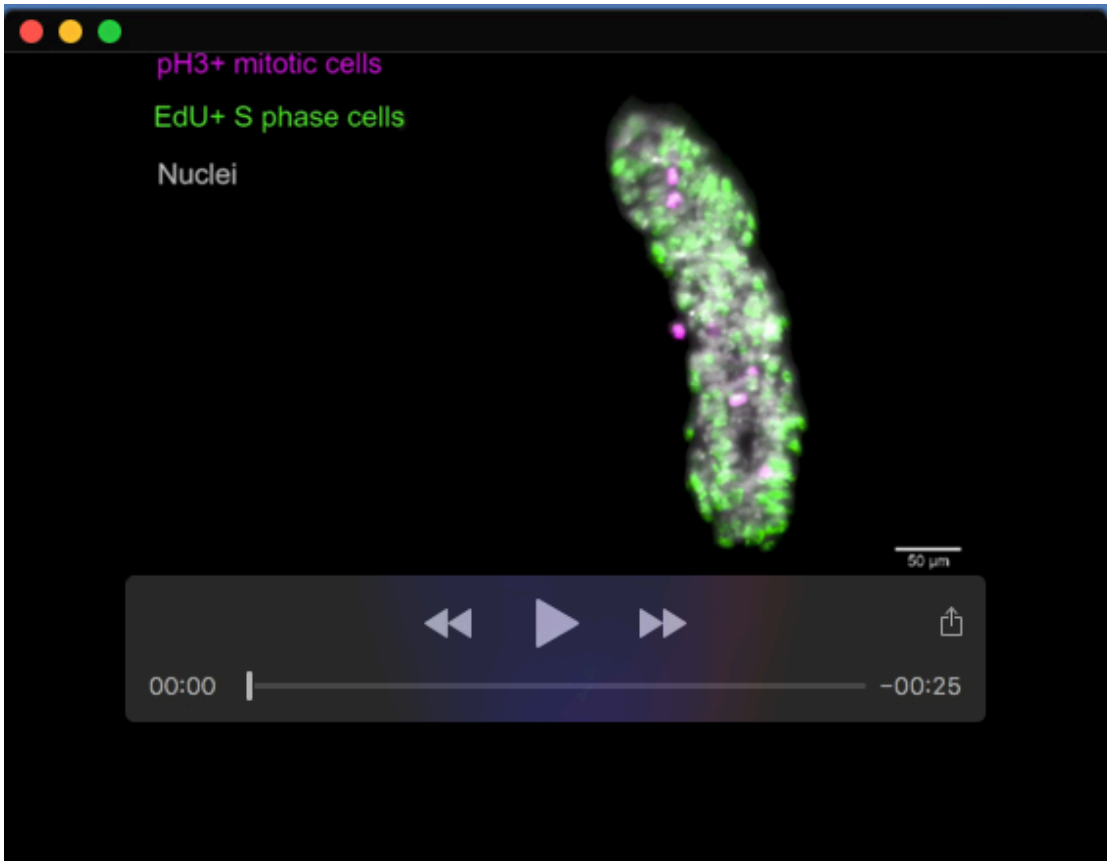


**Movie 4. Interkinetic nuclear migration in the neural tube organoid. Part 1**, The organoids from D6 were stained against $pH3^+$ mitotic cells (magenta) and S phase cells (green) and the images were taken by Zeiss Lightsheet Z1 with 20X clearing objective. In both horizontal axis and longitudinal axis, $pH3^+$ mitotic cells were observed at the apical domain and $EdU^+$ S phase cells were observed at the basal domain of the neural tube organoid. This result implies the interkinetic nuclear migration of the cells in the neural tube organoid. **Part 2**, Time-lapse imaging of the neural tube organoid stained by live cell actin probe with 5 min of interval between D5 and D6 obtained by Visitron CSU-W1 with 60X oil objective. This time-lapse captured the interkinetic nuclear migration of the cells in the neural tube organoid: the cells go to apical domain of the organoid, divide, and reconstitute the epithelium, as the developing neuroepithelial cells do *in vivo*.


**Movie 5. Maturation of the neural tube organoid.** Time-lapse imaging of the neural tube organoids (re-embedded in Matrigel on D6) from D6 to D8 with 1 hour of interval taken by Nikon Eclipse Ti Inverted Microscope with 20X air objective. **Part 1**, the neural crest cells emerge and migrate out from the neural tube organoid. **Part 2**, the neurite extends from the neural tube organoid meaning the emergence of mature neurons.

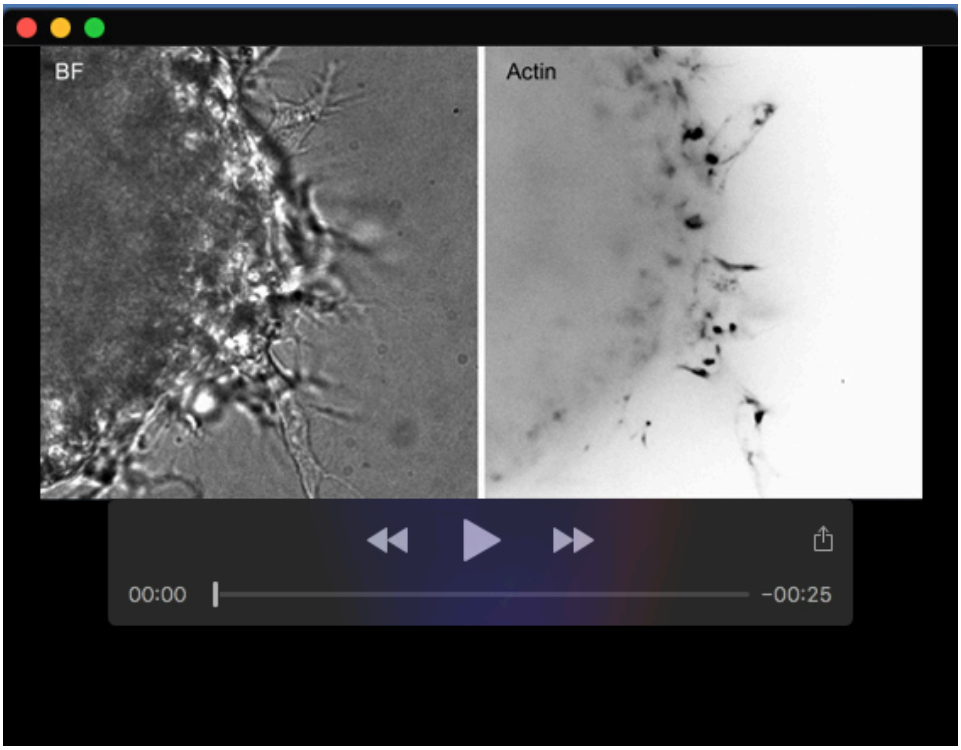


**Movie 6. Neural crest cells: delamination, cell division, and phagocytosis.** Time-lapse imaging of the mature neural tube organoid from D6 to D8 with 5 min of interval by Visitron CSU-W1 with 60x oil objective captured the delamination, cell division, and phagocytosis of neural crest cells derived from neural tube organoid.

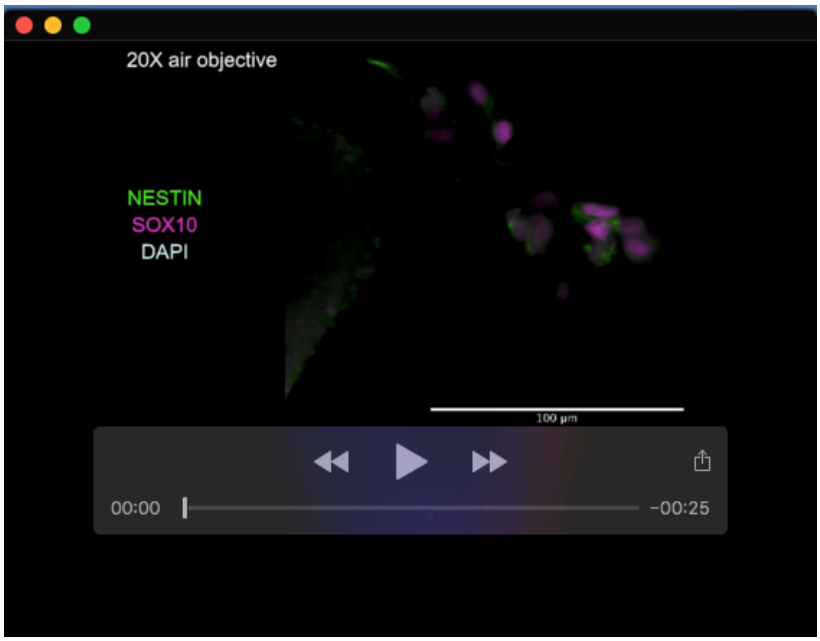


**Movie 7. 3D migration of the neural crest cells.** Confocal imaging of the neural tube organoids (re-embedded in Matrigel on D6 and cultured until D8) with z-stack shows the neural crest cells migrate out from the organoid three-dimensionally. The images were taken by Zeiss LSM700 inversed with 20X air objective and 40X oil objective. The migrating cells outwards from the organoid expressed neural crest cell markers, namely, NESTIN and SOX10. The 3D view of the Z-stack confocal images was processed on IMARIS (Bitplane).

**Table S1. Embedding cell densities**: self-elongating neural tube organoids require the optimal embedding cell numbers of each mESC line

| Cell Line | Cells/10µL Matrigel drop |
|---|---|
| *Sox1*$^{eGFP}$;*Bra*$^{mCherry}$ double reporter (SBr) | 1125 |
| Wild-type of SBr | 1125 |
| *Sox1*$^{GFP}$ reporter | 1000 |
| *Sox10*$^{GFP}$ reporter | 1000 |

## Table S2. Primer sequences used for quantitative PCR

| Probe | Primer Forward | Primer Reverse |
|---|---|---|
| *Oct4* | TGG AGG AAG CCG ACA ACA ATG AGA | TGG TGC CTC AGT TTG AAT GCA TGG |
| *Fgf5* | TCT CCT TTT ATC TGC CCC CT | GAG CAG ATG CAC TCA TTC CA |
| *Otx2* | GCA GAG GTC CTA TCC CAT GA | CTG GGT GGA AAG AGA AGC TG |
| *Sox2* | CAT GAG AGC AAG TAC TGG CAA G | CCA ACG ATA TCA ACC TGC ATG G |
| *Sox1* | AGA CAG CGT GCC TTT GAT TT | TGG GAT AAG ACC TGG GTG AG |
| *Pax6* | CTA CCA GCC AAT CCC ACA GC | TTC GGC CCA ACA TGG AAC |
| *Hoxa2* | CTC GGC CAC AAA GAA TCC CT | GGG GTC TGC AAA GGT ACT TG |
| *Hoxb4* | CAC GGT AAA CCC CAA TTA CGC | CGC GTC AGG TAG CGA TTG |
| *Hoxc4* | AGC ACG GTG AAC CCC AAT TA | GGC GAT CTC GAT CCT TCT CC |
| *Hoxc5* | ATG AGC CAC GAG ACG GAT G | GCG AGT GAG GTA GCG GTT AAA |
| *Hoxc6* | ACA CAC AGA CCT CAA TCG CT | ACC CCA CTG TGC GAA TTC AT |
| *Hoxc8* | GAT GAG ACC CCA CGC TCC T | CTT CAA TCC GGC GCT TTC TG |
| *Hoxc9* | GGA CCC TAG CAA CCC CGT | CGA CGG TCC CTG GTT AAA TAC A |
| *Hoxc10* | GTT TTG GGG TGT TGT GTG TG | TTG CAT GGA GAA CAG AAT GC |
| *Hoxc11* | CCG TCT CTT CCT TCC TAC CC | CGA GTA GCT GTT CCG ATG GT |
| *Hoxc12* | GCG AGT TTC TGG TCA ACG A | TTT TCA TTC TCC GGT TCT GG |
| *Hoxc13* | TCC CTG TTG AAG GCT ACC AG | CTC ACT TCG GGC TGT AGA GG |
| *Lmx1a* | CCC TTG TCT GGA CTC TAC CC | CGG TTG AGT CTA GCT TCC CG |
| *Pax3* | TGC CCA CAT CTC AGC CCT AT | AAT GAA AGG CAC TTT GTC CAT ACT |
| *Pax7* | CGA CTC CGG ATG TGG AGA AAA | TCT GAG CAC TCG GCT AAT CG |
| *Dbx1* | AAG CCC TGG AGA AGA CGT TC | CGC CAT TTC ATG CGT CGA TT |
| *Dbx2* | CCG AAG GAT GAA ATG GCG GA | TGG CTG GGA GAC TTC CCA TA |
| *Nkx6-2* | AGT ATT TGG CAG GCC CAG AG | GCT TCT TTT TAG CCG ACG CC |
| *Olig2* | TTA CAG ACC GAG CCA ACA CC | TGG CCC CAG GGA TGA TCT AA |
| *Nkx2-2* | GGT TCC AGA ACC ATC GCT ACA | TCC ACC TTG CGG ACA CTA TG |
| *Foxa2* | TTT AAA CCG CCA TGC ACT CG | CTC ACG GAA GAG TAG CCC TC |
| *Shh* | ATG TGT TCC GTT ACC AGC GA | ATA TAA CCT TGC CTG CCG CT |
| *Gapdh* | GCA CAG TCA AGG CCG AGA AT | GTG GTT CAC ACC CAT CAC AA |

## Table S3. Primary antibodies used in immunostaining

| Target | Species | Dilution | Cat. No. | Supplier |
|---|---|---|---|---|
| OCT3/4 | mouse | 1:200 | SC-5279 | Santa Cruz Biotechnology |
| SOX1 | goat | 1:20 | AF3369 | R&D Systems |
| PAX6 | rabbit | 1:200 | 901301 | BioLegend |
| CD133/Prominin-1 | rat | 1:200 | 14-1331-82 | Invitrogen |
| SOX2 | rabbit | 1:1000 | ab97959 | abcam |
| T/Brachyury | goat | 1:500 | AF2085 | R&D Systems |
| Phospho-Histone H3 (Ser10) | rabbit | 1:500 | 06-570 | Merck |
| ARL13B | rabbit | 1:200 | 17711-1-AP | Proteintech |
| Acetylated alpha tubulin (Lys40) | mouse | 1:200 | 6-11B-1 | Thermo Fischer |
| NGFR (p75) | mouse | 1:200 | sc-271708 | Santa Cruz Biotechnology |
| BRN3a | rabbit | 1:500 | AB5945 | Merck |
| AP2α | mouse | 1:50 | sc-12726 | Santa Cruz Biotechnology |
| NESTIN | mouse | 1:100 | ab11306 | abcam |
| SOX10 [SP267] | rabbit | 1:25 | ab227680 | abcam |
| TUJ1 | mouse | 1:500 | MMS-435P | Covance |
| GFAP | rabbit | 1:500 | Z0334 | DAKO |
| S100β (EP1576Y) | Rabbit | 1:100 | ab52642 | abcam |
| SM22a | rabbit | 1:200 | ab14106 | abcam |
| ZO-1 | rat | 1:8 | R26.4C | DSHB |
| PKCζ | mouse | 1:200 | sc-17781 | Santa Cruz Biotechnology |
| KI67 (Sp6) | rabbit | 1:200 | MA5-14520 | Invitrogen |
| FOXA2 | rabbit | 1:250 | ab108422 | abcam |
| OLIG2 | rabbit | 1:500 | AB9610 | Millipore |
| Peripherin | rabbit | 1:150 | AB1530 | Millipore |

**Table S4. Secondary antibodies used in immunostaining**

| | Dilution | Cat. No | Supplier |
|---|---|---|---|
| Donkey anti-goat Alexa Fluor 647 | 1:500 | 705-606-147 | Jackson ImmunoResearch |
| Donkey anti-goat Alexa Fluor 488 | | A-11055 | ThermoFisher Scientific |
| Donkey anti-mouse Alexa Fluor 568 | | A-10037 | |
| Donkey anti-rabbit Alexa Fluor 647 | | A-31573 | |
| Goat anti-rat Alexa Fluor 647 | | A-21247 | |
| Donkey anti-rabbit Alexa Fluor 568 | | A-10042 | |
| Donkey anti-mouse Alexa Fluor 647 | | A-31571 | |

**Table S5. Dyes used in staining:** S-phase cell detection, nuclear staining, actin staining, and live cell actin imaging.

| | Dilution | Cat. No | Supplier | Purpose |
|---|---|---|---|---|
| Click-iT™ EdU Cell Proliferation Kit for Imaging, Alexa Fluor™ 647 dye | N/A | C10340 | Invitrogen | S-phase cell detection |
| DAPI | 1:500 | D1306 | Invitrogen | Nuclear dye |
| Alexa Fluor™ 647 Phalloidin | 1:500 | A22287 | Invitrogen | Actin dye |
| sir-actin | 1:1000 | SC001 | Spirochrome | Live cell actin dye |
| BODIPY™ 493/503 | 1:1000 | D3922 | ThermoFisher Scientific | Lipid droplet |

**Table S6. Probe sequences used for whole-mount single-molecule fluorescence *in situ* hybridisation (smFISH)** (Excel file)

Click here to download Table S6

**Table S7. Marker list for cell type of D6 organoids on Figure 2** (Excel file)

Click here to download Table S7

**Table S8. Marker list for cell type of D6-D10 organoids on Figure 4** (Excel file) For cell type identification, we have referenced mainly two single cell transcriptomic analysis reports on developing mouse neural tube: spatial and temporal dynamics of gene expression in spinal cord (Delile *et al.*, 2019) and neural crest development (Soldatov *et al.*, 2019).

Click here to download Table S8